Research Article ISSN 2766-2624

Advances in Earth and Environmental Science

Enhancing Characterization of Reservoirs Within the Niger Delta Basin Using Integration of Seismic and Well Logs

Ndukwe Otobong Sunday[1,2*], Godwin Jeremiah Udom[3] and Charles Ugwu Ugwueze[3]

[1]*World Bank African Centre for Excellence in Oilfield Chemicals Research, Institute of Petroleum Studies, University of Port Harcourt, Nigeria*

[2]*Department of Geology, Federal University of Oye-Ekiti, Oye-Ekiti, Nigeria.*

[3]*Department of Geology, University of Portharcourt, Portharcourt, Nigeria.*

***Correspondence author**

Ndukwe Otobong Sunday
World Bank African Centre for Excellence in Oilfield Chemicals Research
Institute of Petroleum Studies
University of Port Harcourt
Nigeria

Submitted : 26 May 2022 ; Published : 20 June 2022

Citation: N Otobong, Godwin J U and Charles U U. Enhancing Characterization of Reservoirs Within the Niger Delta Basin Using Integration of Seismic and Well Logs.Adv Earth & Env Sci, 2022; 3(2): 1-10.

Abstract

This research utilized well logs and seismic to unravel the reservoir architecture of a field within the offshore depolbelt of Niger Delta. Gamma ray and resistivity log responses were used for lithology and hydrocarbon reservoirs identifications. The principle of similarity in log signatures was used for correlation across the three studied wells. Pertinent reservoir parameters such as shale volume, effective porosity, permeability, hydrocarbon saturation and water saturation were calculated using well-established equations consistent with the geology. Seismic structural interpretation that will give insight to deformation of the field involves the identification and mapping of faults and horizons from seismic sections. By integrating information from seismic and wells, 3D geological modelling was done using geostatistical methods of Sequential Gaussian Simulation and Indicator. The general stratigraphy of the studied field comprises of intercalation of sands and shales which is typical of Agbada formation. Three reservoirs designated as AA, BB and CC were identified and mapped. Only reservoir CC was laterally continuous across the three wells. Reservoir AA has average shale volume of 13%, effective porosity 26%, hydrocarbon saturation 46% and permeability 1328 mD. Reservoir BB has shale volume of 10%, effective porosity 28%, hydrocarbon saturation 43% and permeability 1616 mD. Reservoir CC has shale volume of 21%, effective porosity 20%, hydrocarbon saturation 89% and permeability 580 mD. Twenty faults comprising of both major and minor faults were mapped. The faults mapped were majorly normal faults. The result of the seismic structural interpretation shows that the probable structures harboring oil and gas are a combination of four-way closure and fault assisted anticlinal structures. The modelling of facies and petrophysical parameters into maps aided the understanding of parameter's influence on oil and gas production. Reservoir CC has oil and gas in commercial quantities with 2520 MMcf and 622Mbbls respectively. The result shows the reservoir has high performance system and is therefore recommended for development and production. The resulting models will aid placement of production wells and monitoring of future performance of the reservoirs.

Keywords : Characterization, Quality Ranking, Reservoir Architecture, Stochastic simulation, Hydrocarbon Prospectivity

Introduction

Reservoir characterization pertains to a reservoir system that takes critical information regarding petroleum development and production. Since profit is the key word in oil and gas industry, reducing risk to the bearest minimum made characterization an important phase. Reservoir characterization is a diverse field that aims to identify petroleum deposits and the composition of rocks containing hydrocarbons. In essence, reservoir characterization estimates the gross volume within the trap that has the potential to hold hydrocarbons [1]. In other to map hydrocarbon reservoir, studies of geologic structures that can hold hydrocarbon in place must be considered. The knowledge of reservoir characterization is an important factor in quantifying producible hydrocarbon, it is a method of characterizing the reservoir in terms of petrophysical application using well logs [2]. The predictable and linear physical link between log characteristics and the associated seismic response of underlying rock units is one such approach in use [3]. It can be obtained from well logs especially gamma ray and resistivity logs [4]. The petrophysical determination of reserves has to be done properly before drilling commences so as to consider the risk and the profit involved. Prediction of physical characteristics such as porosity or lithology are examples of quantitative applications [5]. To attain these specified aims, there is a need to conduct geologic and

geophysical investigations that allow engineers to understand the exterior geometry, internal architecture, flow contacts and barriers, aquifer size and lithology variation correspondingly. However, utilizing physical theories, statistical techniques, and geological models, as well as well-log data, we may assess and estimate subsurface characteristics of interest based on the generated results. Nevertheless, uncertainty in seismic interpretation can come from a variety of unavoidable reasons, including inconsistent acquisition circumstances, lateral velocity fluctuation, low data resolution, restricted data availability, insufficient geology understanding, and many more. The economic optimization of reservoir development and hydrocarbon production requires knowledge of reservoir hydrocarbon concentration, recoverability, and recovery time. Importantly, the position and limits of the producing stratum, the continuity of rock strata between neighboring wells, net pay thickness, saturation (oil, gas, and water), and porosity of the reservoir rock are critical information for successful reservoir production performance evaluation. Consequently, this research integrate 3D seismic data and well logs to infer reservoir sand geometry, quantify their thicknesses and depths, assess their petrophysical characteristics, and estimate their volumetric contents.

Location of the study Area Geology

Bong field is located within the Niger Delta basin of Nigeria (Fig. 1a). The Niger Delta has played a significant role in boosting the country's and neighboring countries' economies through the use of substantial petroleum reserves. Several writers have contributed to the knowledge of the Niger Delta basin's sedimentology, tectonics, stratigraphy, depositional environment, petrophysics, and hydrocarbon potential. The following authors have written about them [6-13]. The Niger Delta is located near the Gulf of Guinea in West Africa [6]. The Niger Delta sub-aerial segment stretches over roughly 75000 km2 and encompasses approximately 200 km from peak to entrance. The complete sedimentary prism encompasses 140000 km2, with a highest stratigraphic thickness of approximately 12 km [14]. The wide sedimentary order stratigraphy is split into three lithostratigraphic units, namely the Akata, Agbada, and Benin Formations [6]. The uppermost unit, the Benin Formation starting from Eocene to latest era includes continental/fluviatile deposits of up to 2500 m dense sands, gravels and back swamps, underlying the Benin Formation is the Agbada formation. These are predominantly interbedded sandstones and shale organized into coarsening upward "offlap" cycles with minor lignite. This unit is underlain by the Akata Formation, which spans the Paleocene to the most recent epoch and has up to 6500 m of marine clay with silty and sandy interbeds [14]. They are regarded as a mobile substratum comparable to natural evaporites that deforms in reaction to deltaic programming and sedimentary loading [10]. The depobelts are divided into seven east-westbound blocks that correlate with the individual moments of the event record of deltas ranging from the foremost mature within the northern delta to the immature offshore in the south. It is well acknowledged that each depobelt consists of a more or less unique segment on sedimentation, structural deformation, and therefore the creation and accumulation of hydrocarbons [9].

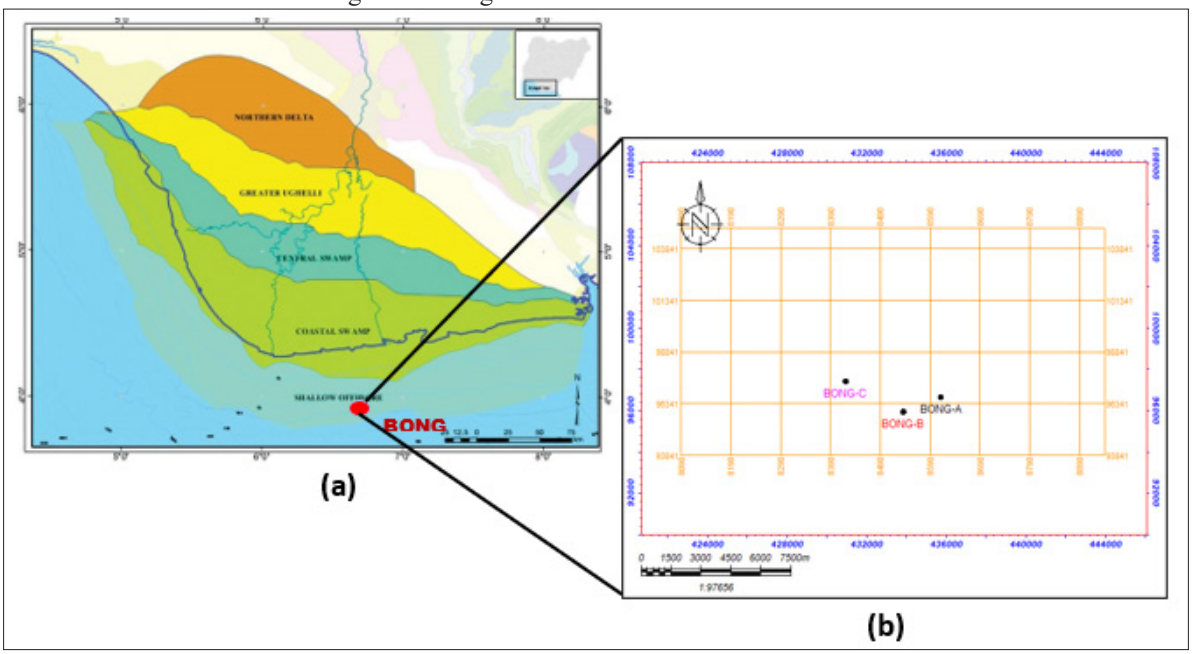

Figure 1: Location of the study area (a) Niger Delta Map showing the different depobelts and study location (Red Ellipse) modified after Bolaji 2020. (b) Base map of BONG Field showing the positions of wells and seismic lines.

Niger Delta Petroleum System

Petroleum is found in the Agbada Formation in the Niger Delta clastic wedge [15,16]. The distribution of hydrocarbons shows a general tendency for the ratio of gas to grease to extend southward within individual depobelts [17]. Stacher (1995) developed a hydrocarbon habitat model based on the stratigraphy of a few petroleum-rich belts in the Niger Delta area [18]. Gas to grease ratios within reservoirs were reported by Evamy *et al* (1979), Ekweozor and Okoye (1980), Ejedawe (1981), Bustin (1988), Doust

and Omatsola (1990), Owoyemi (2004), Owoyemi (2005) and Onwuchekwa (2017). Tuttle et al. (1999) assumes that belts roughly correspond to the transition between continental and oceanic crust within the axis of maximum sediment thickness [9,10,12,16,19-22]. The Niger Delta's source rocks are primarily marine interbedded shale in the Agbada Formation, marine Akata Formation shales, and underlying Cretaceous shales [12,23-27]. Reservoir intervals in the Agbada Formation are thought to represent highstand and transgressive system tract deposits in proximal shallow ramp environments (Evamy et al., 1978; Udoh, 2020). The reservoirs vary in thickness from below 45 feet to a few with thicknesses above 150 feet [9,28]. Kulke (1995), Tuttle et al (1999) and Alabi (2019) describes the foremost important reservoir units as point bars of distributary channels and coastal barrier bars intermittently cut by sand filled channels [12,15,29]. Most major reservoirs were considered to be Miocene-aged paralic sandstones with a porosity of 40%, a permeability of 2 Darcy, and a thickness of around 300 feet [16,22,30,31]. Reservoir units have different grain size; fluvial sandstones tend to be coarser than the delta front sandstones. Point bar deposits fine upward; barrier bar sandstones tend to possess the simplest grain sorting [15]. The bulk of the sandstones are unconsolidated, with only little argillaceous and siliceous cement. Deep-channel sands, lowstand sand masses, and proximal turbidite sandstones are examples of potential reservoirs in the delta complex's outer reaches [11].

Materials and Methods

The data set available for this research consists of a base map, a three-dimensional seismic volume, suites of well logs from three wells and a checkshot. The dataset was provided by Shell Petroleum Development Company (SPDC) Nigeria. The 3D seismic data is a post stack migrated having area coverage of 234 km2. It consists of 852 inlines and 441 crosslines. Fig. 1b shows the distribution and orientation of both the seismic and well logs dataset. The datasets were majorly enhanced, processed and analysed using petrelTM software. The method of study includes qualitative interpretation, quantitative interpretation, seismic structural interpretation, 3D reservoir modelling and volumetric estimation.

Qualitative Interpretation

Qualitative log interpretation involves the use of well log data such as gamma ray, deep resistivity, density and neutron log for the identification of lithology within the three wells. Gamma ray log was principally used for the identification of major lithologies within the study field. Clean sand and shale baseline was established at a cut-off mark of 73 API. The sand baseline depicts minimum gamma ray response while the shale baseline depicts maximum gamma ray response. Gamma ray values less than 73 API was interpreted to be sand units while higher values greater than the cut-off was interpreted to be shale units. Three hydrocarbon bearing reservoirs were identified using true resistivity logs that measures the true resistivity of a formation. High resistivity readings corresponding to low gamma ray values was interpreted to be probable hydrocarbon bearing units. Combination of density and neutron logs were used to identified contact and fluids type present in the three delineated reservoirs. Two major hydrocarbon type (gas and oil) were identified on the basis of pattern resulting from crossover of neutron and density logs. Reservoir AA and BB are oil saturated while reservoir CC has combination of gas and oil. Contacts (gas-oil contact, oil-water contact) useful for the estimation of reserves was achieved by exploiting crossover of neutron and density logs.

Quantitative Interpretation

This involves the estimation of physical properties of the delineated reservoirs from established equations. Some calculated parameters include volume of shale, porosity, permeability, water and hydrocarbon saturations. Volume of shale (V_{sh}) was mathematically calculated after gamma ray index (IGR) of the shally sand was determined. The index was calculated using the eq. (1) below:

$$I_{GR} = \frac{(GR_{log} - GR_{min})}{(GR_{max} - GR_{min})} \quad (1)$$

Where, GR_{max} is gamma ray log reading in 100% shale, GR_{min} is gamma ray log reading in 100% clean sand zone, GR_{log} is gamma ray log reading in the zone of interest (Reservoirs).

Volume of shale was then estimated using relationship of Dresser Atlas (1979) formulae for tertiary and unconsolidated rocks stated below [32]:

$$V_{sh} = 0.083*[2^{3.7 \times I_{GR}} - 1.0] \quad (2)$$

Porosity was calculated using average porosity (eq. 4) gotten from both density and neutron logs as contained in Dresser Atlas (1979) [32]. Porosity from density (ΦD) was computed using the equation below:

$$\Phi_D = \frac{\rho_{ma} - \rho_b}{\rho_{ma} - \rho_{fl}} \quad (3)$$

Where, p_{ma} is the matrix density (2.65 gm/cm^3 for sandstone unit), p_{fl} is the fluid density and p_b is the formation bulk density.

Porosity neutron (Φ_N) was gotten and corrected for using neutron log. Average porosity (Φ_{AVG}) was calculated using eq. (4) :

$$\Phi_{Avg} = \sqrt{\frac{\phi^2 D + \phi^2 N}{2}} \quad (4)$$

Effective porosity (Φ_{eff}) which measure the total volume of a reservoir that consist interconnected voids was calculated using eq. (5) below:

$$\Phi_{eff} = \Phi_{Avg} \times (1 - V_{sh}) \quad (5)$$

Formation factor (F) was calculated using eq. (5):

$$F = \frac{a}{\phi^m} \quad (6)$$

Where a is tortuosity factor (1), m is cementation factor (2.15) and ϕ is porosity.

Irreducible water saturation (S_{wirr}) was estimated using:

$$S_{wirr} = \sqrt{\frac{F}{2000}} \quad (7)$$

Where F is the Formation factor.

Permeability was calculated Tixier (1956) relationship [33]. It is given by:

$$K = \sqrt{\frac{250 \times \phi 3_{eff}}{S_{w\,irr}}} \quad (8)$$

Where Φ is porosity, Sw_{irr} is the irreducible water saturation. Water saturation (S_w) for the uninvaded zone was determined using Archie's equation (1942) given below [34]:

$$S_w^2 = \frac{F \times R_w}{R_t} \quad (9)$$

Hydrocarbon saturation (Sh) was estimated using in eq. (10) below:

$$S_h = (100 - S_w)\ \% \quad (10)$$

Seismic Structural Interpretation

Seismic interpretation was performed using a realized volume. Geologic discontinuities such as faults were identified and mapped based on the abrupt gradual and subtle changes of amplitudes. Twenty faults (20) were identified and mapped across the field (Fig. 2).

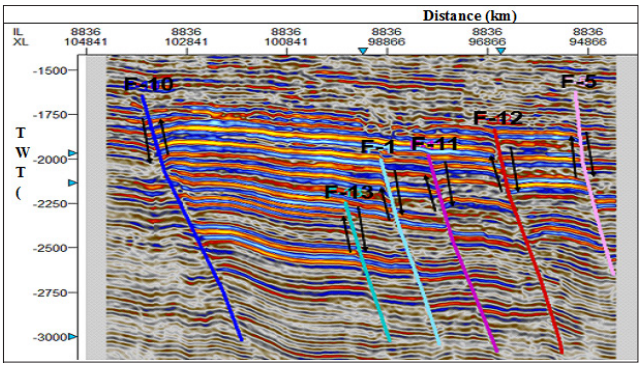

Figure 2: Structural Interpretation of Fault on Inline 8836

They are majorly growth faults and roll-over anticline. Faulting plays important role in the understanding of juxtaposition of lithologies. The juxtaposition of reservoir sands against shale beds due to faulting usually creates good seal integrity. Three key horizons representing the top of reservoirs were tied with the seismic volume. This was done by creating synthetic seismogram from the convolution process of reflection coefficient series and representative wavelet. All the three tops corresponded to the troughs and this suggest the reservoir sand units are low impedances. Tied horizons were mapped across both inlines and crosslines which were used in the generation of time structural maps (Fig. 3). A velocity model was built from polynomial second order equation using checkshot data (Fig. 4). This model was used in the conversion of time structural maps to depth equivalents [35].

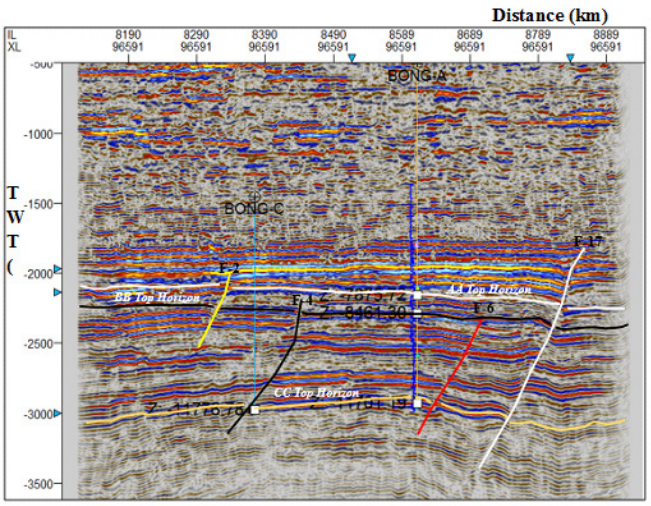

Figure 3: Typical Interpreted Section showing Well tops and Mapped Horizons

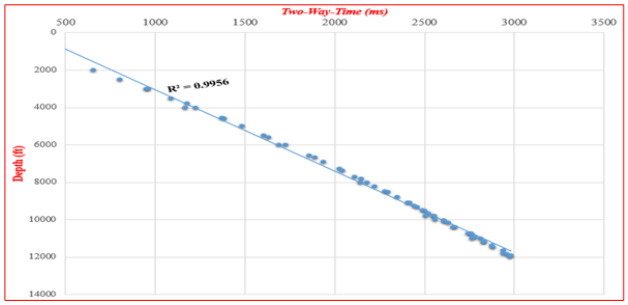

Figure 4: TWT-Depth Curve using Polynomial fitting

3D Reservoir Modelling

Characterization and modeling of the delineated reservoirs was carried out utilizing wells and seismic datasets. The exploration and production phases typically reliant on the subsurface information derived from wells and seismic to model resolution (element scaling), facies and petrophysical modellings. Petrophysical parameters modeled include net-to-gross, effective porosity, permeability, water and hydrocarbon saturations. The structural framework forms the main background to the model using the results from structural interpretation of 3D seismic data. Model scaling through pillar gridding was done with grid size I, J, K (203*105*25). The grid size was carefully selected in order for the model to capture relevant stratigraphic and elemental heterogeneity of the reservoir zones. Modeling variogram analysis was carried to quantitatively describe the variation of how field data varies as a function of distance between data points. The analysis was carried out using primary data (well log) along the vertical direction for all the zones. Variogram and distribution were effectively used to create local variability away from input data. The choice of modeling algorithm for populating of discrete parameters was carefully done for the process of Stochastic simulation. Sequential Gaussian Simulation and Sequential Indicator Stimulation which honor the well data, input distributions, variogram and trends were used for facies and petrophysical modeling respectively. The Stochastic simulation gave the multiples representations to characterize uncertainties.

Volumetric Estimation

Model based volume estimation was used in the computation of the reserve within the three delineated reservoirs. The contacts identified were useful in the calculation of areas. Net-to-gross, porosity, water saturation and facies models were used in the estimation. Original Oil and gas initially in place and ultimate recovery of the volumes were estimated. Recovery factor of 0.45 was used for the calculation. The computation was done using the equation below:

$$STOIIP = \frac{GRV * NTG * \Phi eff * (1 - SW)}{BO} \quad (11)$$

$$UR = STOIIP * R_f \quad (12)$$

Where, STOIIP is stock tank oil initially in place. UR is ultimate recovery, GRV is gross rock volume (Area*Gross thickness), NTG is Net-to-gross, Φ_{eff} is effective porosity, S_w is water saturation, Boi is formation volume factor for oil, Bg is formation volume factor for gas and R_f is recovery factor.

Results and Discussion

Qualitative Interpretation

Lithological interpretation results revealed the major lithologies units as sand and shale (Fig. 5). It is typical of Agbada Formation stratigraphy. Sands unit is a potential reservoir rock and shale unit a potential seal and source rock. Three delineated reservoirs designated as AA, BB and CC show low value of water saturation and high value of hydrocarbon saturation. Lithostratigraphic correlation of the identified reservoirs along North-west-South-east direction (Fig. 6) revealed structural disposition that has affected the study field. Reservoir CC was laterally continuous across the three wells. Exploiting the crossover of neutron and density logs, Reservoir AA and BB contain oil while Reservoir CC contains combination of gas and oil.

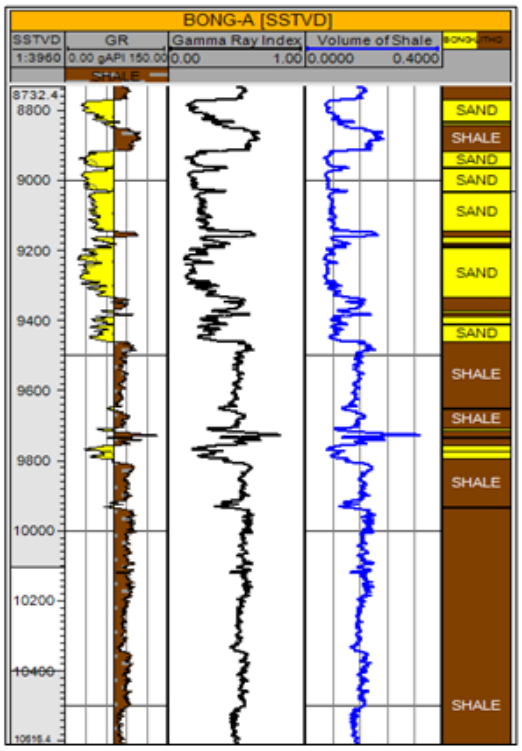

Figure 5: Lithological Interpretation within the Study Field

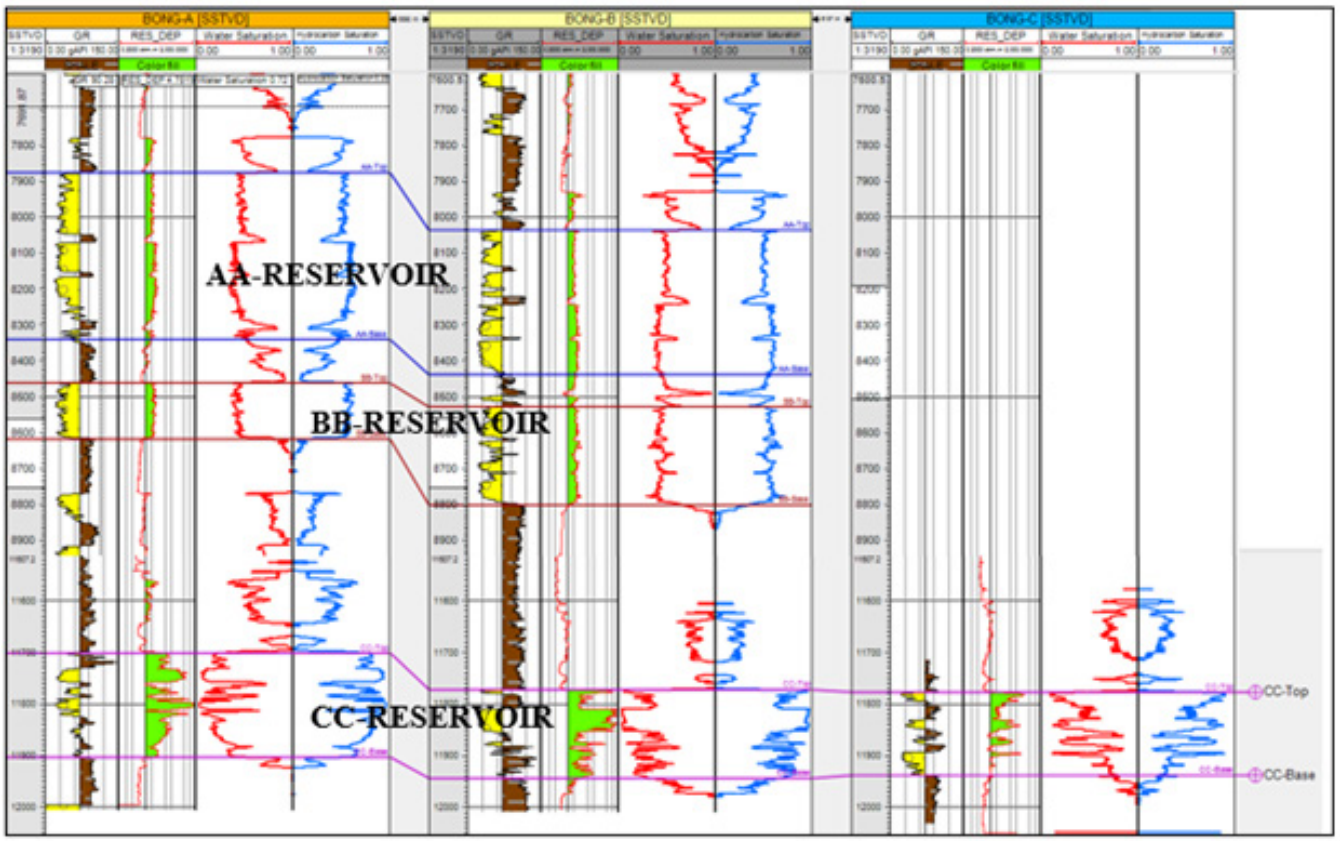

Figure 6: Lithostratigraphic Correlation of the Reservoirs across the Three Wells

Quantitative Interpretation

Petrophysical attributes of the delineated reservoirs which will further help in further decision was done using well-established equation consistent with the geology of the study field. Reservoir AA is located within the depth range of 2400-2563m, reservoir BB 2578-2668 m and reservoir CC 3566-3639 m across the wells. The average petrophysical parameters is summarized in table 1.

Petrophysical Parameters	Reservoir AA	Reservoir BB	Reservoir CC
Gross thickness(m)	135	65	55
Net sand thickness(m)	117	62	32
NTG	87	97	57
I_{GR}(%)	31	29	46
V_{sh}(%)	13	10	21
Porosity (ϕ_{AVG}) (%)	29	30	23
Effective porosity (ϕ_{eff})(%)	26	28	20
Permeability(mD)	1328	1616	580
S_w(%)	54	57	11
S_h(%)	46	43	89

Table 1: Computed Average Petrophysical Parameters of the three Reservoirs

Reservoir AA has average gross thickness of 135m, net sand thickness 117 m, net-to-gross 87%, shale volume 13%, effective porosity 26%, permeability 1328 mD and hydrocarbon saturation 46%. Reservoir BB has average gross thickness of 65 m, net sand thickness 62 m, net-to-gross 97%, shale volume 10%, effective porosity 28%, permeability 1616 mD and hydrocarbon saturation 43%. Reservoir CC has average gross thickness of 55 m, net sand thickness 32m, net-to-gross 57%, shale volume 21%, effective porosity 20%, permeability 580 mD and hydrocarbon saturation 89%. Fig. 7 is a statistical petrophysical analysis of the three reservoirs. The representation shows that reservoir BB has the highest net-to gross, lowest shale volume, highest effective porosity and lowest hydrocarbon saturation. Similarly, reservoir CC has better ranking of the three reservoirs. It is characterized with good porosity and permeability suggesting free flow of hydrocarbon within the reservoir. The reservoir also contain high hydrocarbon saturation at irreducible water saturation. This suggest that reservoir CC is more prolific and good for hydrocarbon exploitation than the other two reservoirs.

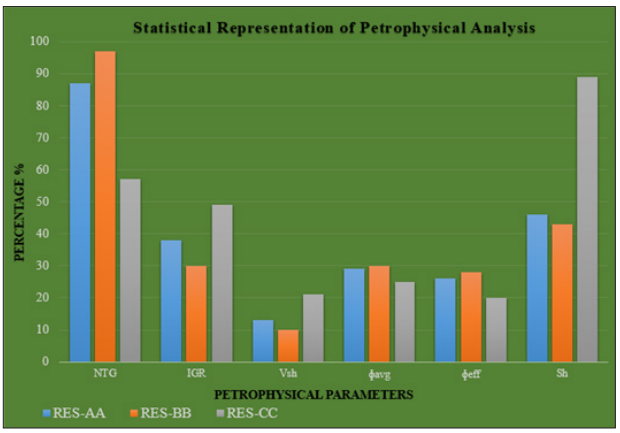

Figure 7: Statistical Petrophysical Analysis

Seismic Structural Interpretation

Fault interpretation was carried out on all the inlines. Seven of the twenty faults mapped within the study are major growth faults and thirteen were minor which are synthetic and antithetic to the major. The result affirmed that the study field has undergone deformation or tectonic activities. Three horizons corresponding to the top of the three identified reservoirs on the well logs after properly tied with seismic were mapped across the seismic volume. The horizon grids were used to produce time structural maps. Depth structural maps that show the true position of structures and faults within the subsurface were also generated using appropriate velocity model. Fig. 8, 9, 10 (a) and (b) are time and depth structural maps of reservoir AA, BB, and CC tops respectively. Reservoir AA time structural map has time variation of 2.10 to 2.3 milliseconds with depth equivalent contour lines varies from -7.2 to -8.4km. Reservoir BB time structural map has time variation of 2.13 to 2.5 milliseconds with depth equivalent contour lines varies from -7.8 to -8.5 km. Reservoir CC time structural map has time variation of 2.9 to 3.3 milliseconds with depth equivalent contour lines varies from -11.4 to -13.8km. The structurally high areas on the maps are found at the northeastern and central parts where the existing wells are located. This affirmed the validity of the existing interpretation carried out on the field. The polygons of the mapped faults revealed the extent of structural disposition in the location of existing wells. The depth structural maps take almost the same structures as those of time structural maps which implies the appropriateness of the velocity model used in the conversion. It can be observed from the maps that the probable trapping mechanism responsible for hydrocarbon accumulations is fault assisted anticlinal structure that can serve as seal to prevent further hydrocarbon migration.

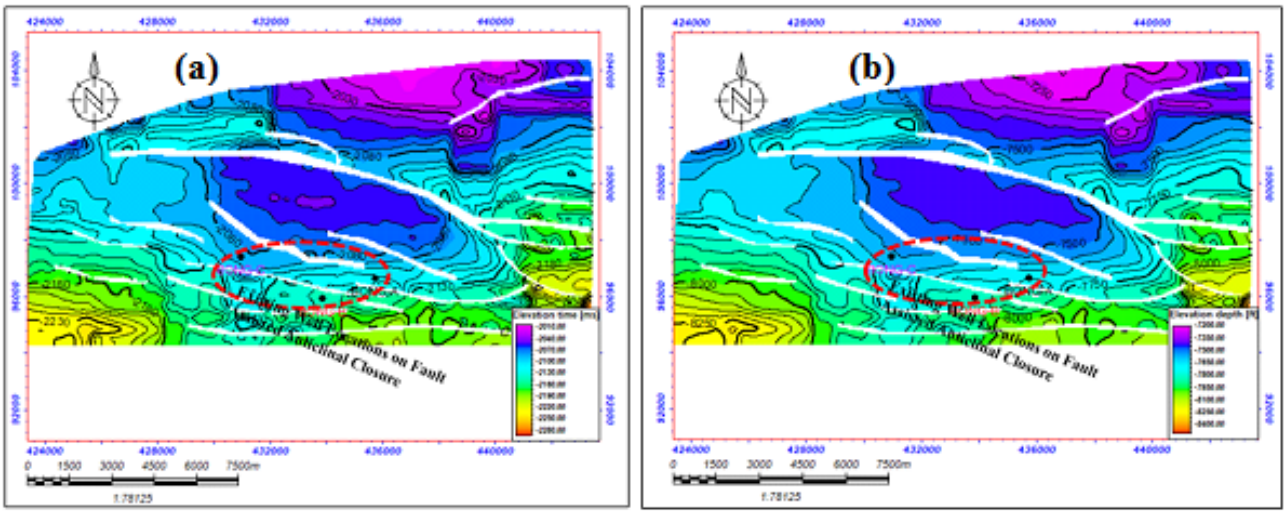

Figure 8: (a) Time Structural Maps of Reservoir AA Top. (b) Depth Structural Maps of Reservoir AA Top

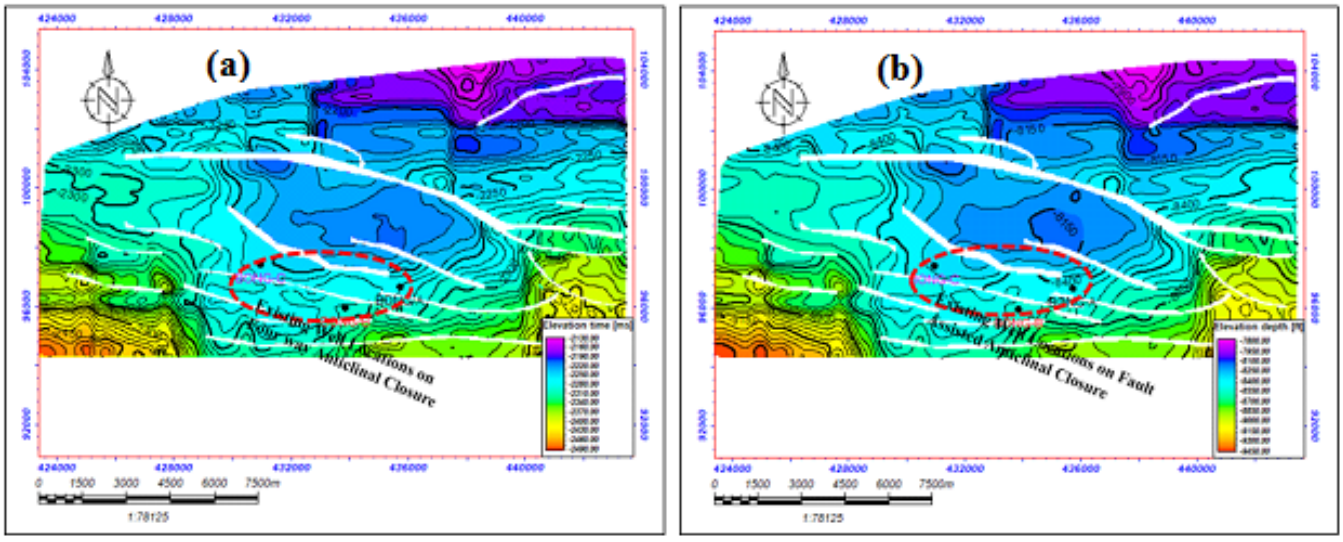

Figure 9: (a) Time Structural Maps of Reservoir BB Top. (b) Depth Structural Maps of Reservoir BB Top

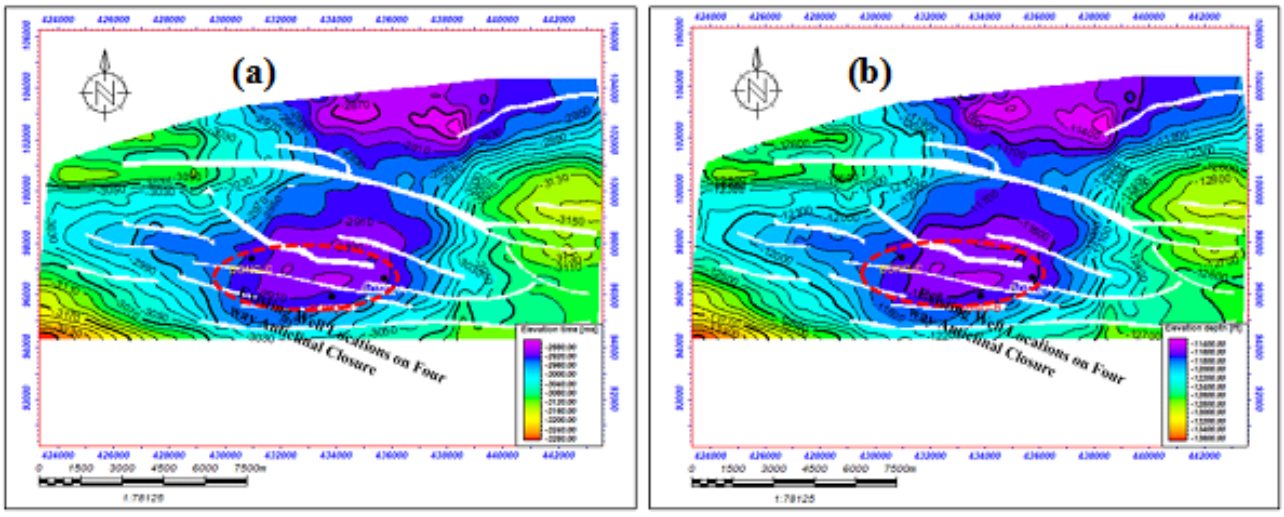

Figure 10: (a) Time Structural Maps of Reservoir CC Top. (b) Depth Structural Maps of Reservoir CC Top

3D Reservoir Models

Fig. 11 shows the gridding result which comprises of the top, mid, and base skeleton which serve as structural framework for reservoir modelling. The results revealed that geological heterogeneities of reservoirs will be captured with grid resolution for the construction of the geological model. Nine (9) faults cutting across the existing well locations were modelled. The result (Fig. 11) shows that the major faults are dipping toward the northwestern part of the field while the minor faults are antithetic to the major faults.

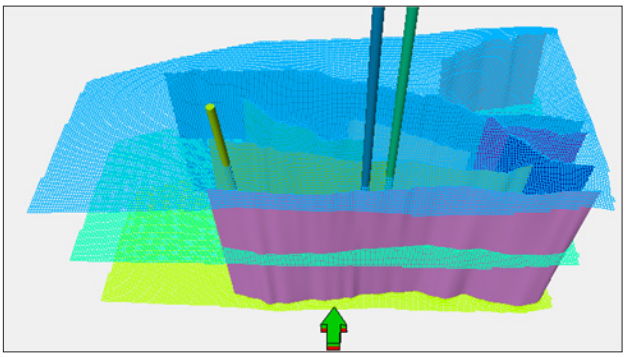

Figure 11: Pillar Gridding capturing Skeletal Framework (top, mid and base) and modeled Faults

Fig. 12 is a lithofacies model of reservoir CC. The result revealed the distribution of major lithologies within the study field. Higher proportion of sand units are well distributed in the northern and central part. This affirmed the existing interpretation. The result also suggest that the reservoir has high connectivity of sand which will allow easy fluid flow. Fig. 13 shows the reservoirs juxtaposition model along a fault (F-1). The result shows the juxtaposition against shale on the fault plane and this sealed up the fault plane from leaking. This implies that the reservoir CC is relatively sealed because shale-on-sand, or sand-on-shale juxtaposition has high sealing potential.

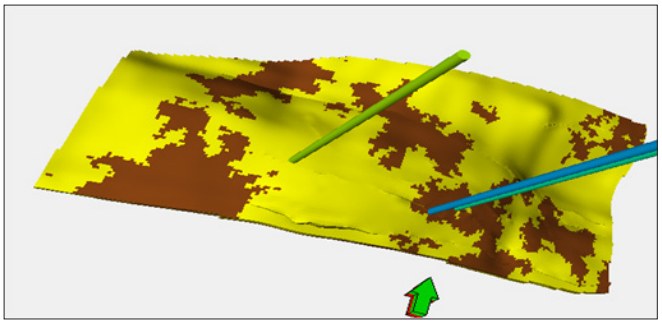

Figure 12: Lithofacies Reservoir Model

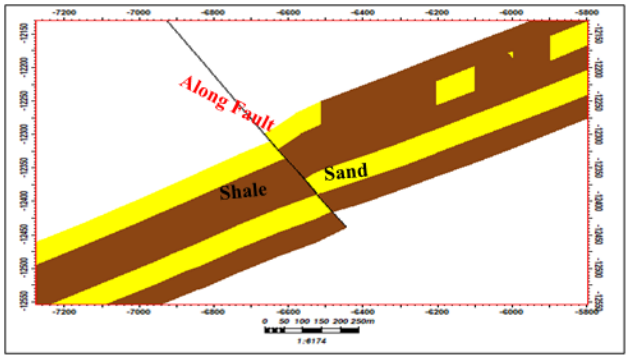

Figure 13: Stratigraphic Juxtaposition Map along Fault F-1

The process of building petrophysical property models helps in the assigning of petrophysical properties of estimated values to each cell of the 3D grid. Fig. 14 is the net-to-gross (NTG) model. The result revealed the distribution of high sand-to-shale ratio ranges from 0.55 to 0.9. This distribution is a good indicator for high hydrocarbon prospectivity within the study area. Fig.15 and 16 are effective porosity and permeability models respectively. Effective porosity and permeability are important reservoir interconnectivity indicators. The modelling results show that the pore spaces within the reservoir are interconnected and thus fluid can flow easily and extracted within the connected pore spaces during the oil and gas exploitation.

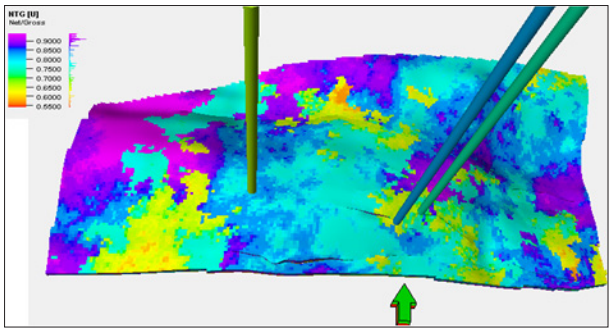

Figure 14: Net-to-Gross Reservoir Model

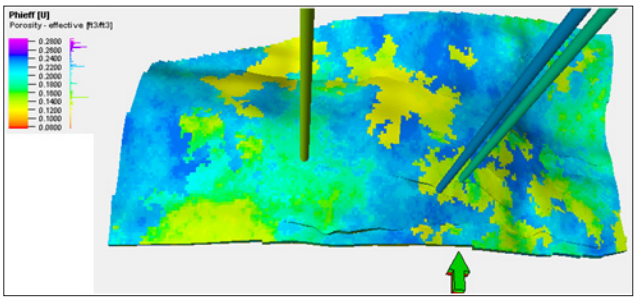

Figure 15: Effective Porosity Reservoir Model

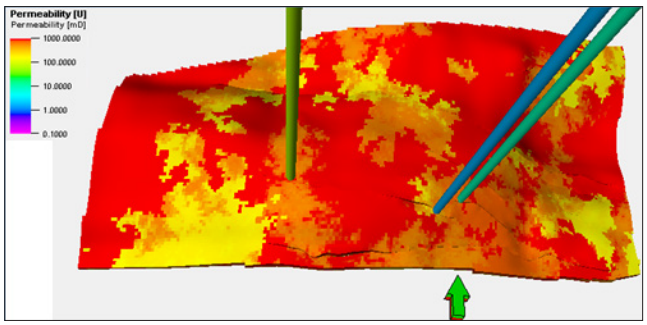

Figure 16: Permeability Reservoir Model

Water saturation model (Fig. 17) and hydrocarbon saturation model (Fig. 18) give the distribution of fluid types within the study field. Generally, low water saturation corresponds to high hydrocarbon saturation. Low water saturation was generally observed at the location of existing wells, northern and central parts of the field. This gives high hydrocarbon accumulation indication within the delineated reservoir. The high hydrocarbon saturation in the northern and central parts of the field suggest the regions can be focused on for the citation of more development wells.

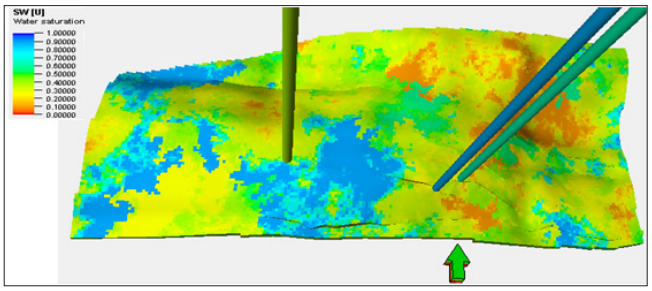

Figure 17: Water saturation Reservoir Model

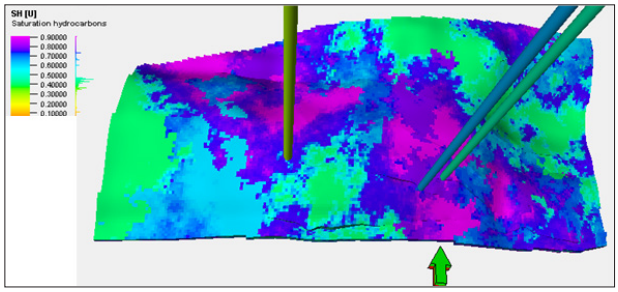

Figure 18: Hydrocarbon saturation Reservoir Model

Volumetric Results

The volume of hydrocarbon original in place and the volume that can be recovered were estimated in each reservoir. Table 2 shows the summary of the result. The ultimate recoverable volume results shows that AA has 410 MMbbls reservoir BB 590 MMbbls and reservoir CC has 2530 MMcf and 622 MMbbls respectively. This shows that reservoir CC has great hydrocarbon potential of considerable volume than other two reservoirs analysed which can be exploited for commercial purpose. The results also agreed with petrophysical ranking.

Volumemetric Parameters	Reservoir AA	Reservoir BB	Reservoir CC
Area (Acres)	1570	2405	6896
Gross thickness(m)	135	65	55
Net sand thickness(m)	117	62	32
NTG	0.87	0.97	0.57
Effective porosity (ϕ_{eff})	0.26	0.28	0.20
S_w	0.54	0.57	0.11
Bulk Volume (*106 ft^3)	26525	39989	26867
UR_{gas} (MMcf)	-	-	2530
UR_{oil}(MMbbls)	410	590	622

Table 2: Volume Estimation of the three Reservoirs

Conclusion

The study provided the effectiveness of integrated approaches in enhancing characterization of reservoirs within the offshore settings for optimum production. Two major lithologies delineated revealed that sand units are potential reservoir rock that can accumulate oil and gas while shale units are potential source rocks or seals. Quantitative analysis of the three identified reservoirs showed reservoir CC has better quality ranking than the other two reservoirs. Seismic structural interpretation confirmed deformation and tectonic activities that had occurred in Niger Delta basin as reported by several authors. The result showed that the trapping mechanism of hydrocarbon is four-way and fault assisted anticlinal structures. Fault model result provided direction of the major faults and the implication to oil and gas production. Facies model showed the high connectivity corresponding to low amalgamated of sand units especially at the northern and central parts of the study field. This is an important result for the production engineers in the citation of production wells. The juxtaposition revealed the sealing capacity of the reservoirs. Petrophysical models showed the distribution of reservoir properties (NTG, effective porosity, permeability, water and hydrocarbon saturations) across the field. Regions with high NTG, porosity, permeability, hydrocarbon saturation and low water saturation are always good prospective zones. The volumetric estimation confirmed the petrophysical results that reservoir CC possesses the best quality ranking and hence should be the uttermost target for exploitation within BONG field. Citation of more development wells should also be targeted at the northern and central parts of the study field as affirmed by the integrated results.

Acknowledgement

The authors appreciate Shell Petroleum Development Company (SPDC) Exploration for making the dataset available for this research work.

References

1. Eshimokhai S, Akhirevbulu O (2012) Reservoir Characteristics using Seismic and Well Logs Data (A Case Study of Niger Delta): EJESM 5.
2. Schlumberger (1989) Log interpretation, Principle and Application: Schlumberger Wireline and Testing, Houston, Texas, 21-89.
3. Muslime BM, Moses AO (2011) Reservoir Characterization and Paleo-Stratigraphic imaging over Okari Field, Niger Delta using neutral networks: The Leading Edge, 1: 650 655.
4. Asquith G (2004) Basic Well Log Analysis. American Association of Petroleum Geologists, Methods in exploration series: Assoc Pet Geol Bull 16: 12-13.
5. Sagan J and Hart B (2006) Three Dimensional Seismic-based Definition of Fault-related Porosity Development, AAPG Bulletin 90: 1763-1785.
6. Short KC, Stauble AJ (1967) Outline of Geology of Niger delta: Assoc Pet Geol Bull 51: 761-779.
7. Weber KJ, Daukoru EM (1975) Petroleum Geology of the Niger Delta: Proceedings of the Ninth World Petroleum Congress, Vol 2, Geology London, Applied Science Publishers, Ltd 210-221.
8. Avbovbo AA (1978) Tertiary lithostratigraphy of Niger Delta: Assoc Pet Geol Bull 62: 295-306.
9. Evamy BD, Haremboure J, Kammerling R, Knaap WA, Molloy FA (1978) Hydrocarbon habitat of tertiary Niger Delta: AAPG Bulletin 62: 1-39.
10. Doust H, Omatsola E (1990) Niger delta: in J. D. Edwards and P.A. Santogrossi, eds., Divergent/passive margin basins: AAPG Memoir 48: 239-248.
11. Beka FT, Oti MN (1995) The distal offshore Niger delta: frontier prospects of a mature petroleum province, in Oti, M.N., and G. Postma, eds., Geology of deltas: Rotterdam, A. A. Balkema 237-241.
12. Tuttle MLW, Charpentier RR, Brownfield ME (1999) The Niger delta petroleum system: Niger delta province, Nigeria, Cameroon, and Equatorial Guinea, Africa: USGS Open-file report 99-50-H.
13. Reijers TJA (2011) Stratigraphy and Sedimentology of the Niger Delta. Geologos 17: 133- 162.
14. Bolaji TA (2020). Reservoir Souring Possibilities in Freeman Oilfield, Niger Delta: Insights from Mineralogy, Diagenesis and Water Chemistry. PhD Thesis of the University of Port Harcourt, Nigeria.
15. Kulke H (1995) Nigeria, in H. Kulke, ed., Regional petroleum geology of the world. Part II: Africa, America, Australia and Antarctica: Berlin, Gebruder Borntraeger 143-172.
16. Owoyemi AO (2005) Sequence Stratigraphy of Niger Delta, Delta Field, Offshore Nigeria.
17. Doust H (1989) The Niger delta: Hydrocarbon potential of a major Tertiary delta province, in coastal lowlands, geology and geotechnology, in Proceedings of the Kon. Nederl. Geol. Mijnb. Genootschap 203-212.
18. Stacher P (1995). Present understanding of the Niger delta hydrocarbon habitat, in Oti, M. N. and Postma, G., eds.,Geology of deltas: Rotterdam, A.A. Balkema 257-267.
19. Ekweozor CM and Okoye NV (1980) Petroleum source-bed evaluation of Tertiary Niger Delta: AAPG Bulletin 64: 1251-1259.
20. Ejedawe JE (1981) Patterns of incidence of oil reserves in Niger delta basin AAPG Bulletin 65: 1574-1585.
21. Bustin RM (1988) Sedimentology and characteristics of dispersed organic matter in Tertiary Niger delta: Origin of source rocks in a deltaic environment: Assoc Pet Geol Bull 72: 277-298.
22. Onwuchekwa C (2018) "Application of Machine Learning Ideas to Reservoir Fluid Properties Estimation." Paper presented at the SPE Nigeria Annual International Conference and Exhibition, Lagos, Nigeria.
23. Mattick RE (1982) Assessment of the Petroleum, Coal and Geothermal Resources of the Economic Community of West African States.
24. Odumodu FC (2011). Geothermal gradient and heat flow variations in parts of the eastern Niger Delta, Nigeria: Journal of the Geological Society of India 88: 107-118.
25. Falebita DE (2015) A Study of the Organic Richness and Petrophysical Characteristics of Selected Shales from Niger Delta: IJS 17.
26. Oluwajana OA, Ehinola AO and Okeugo CG (2017). Modeling hydrocarbon generation potentials of Eocene source rocks in the Agbada Formation, Northern Delta Depobelt, Niger Delta Basin, Nigeria J. Pet. Technol 7: 379-388.
27. Ilevbare M, Omorogieva OM (2020) Formation evaluation of the petrophysical properties of wells in e - field onshore Niger Delta, Nigeria: Nigerian Journal of Technology, 39: 961-971.
28. Udoh AC, Bassey CE, Ekot, AE, and Udoh MU (2020) Sequence stratigraphicstudy of â€˜Xâ€™ field in eastern offshore of Niger Delta, Nigeria: J Geo Min Res 12: 65-79.
29. Alabi AA (2019) Geology and Environmental Impact Assessment and Benefit of Granitic Rocks of Minna Area, Northwestern Nigeria EJESM 4: 201.
30. Edwards JD and Santogrossi PA (1989) Summary and conclusions, in, Edwards, J.D., and Santogrossi, P.A., eds., Divergent/Paaive Margin Basins, AAPG Memoir 48: Tulsa, American Association of Petroleum Geologists 239-248.
31. Ojo AO (2016) Geophysical Investigation for Groundwater Potential and Aquifer Protective Capacity: America. Journal of Water Resources 4: 137-143.
32. Dresser A (1979) Log interpretation chart. Houston Dresser Industries, Inc 107.
33. Tixier MP (1956) Fundamentals of electrical logging—microlog and microlatero1og. In: Fundamentals of logging. Petroleum Eng. Conf. Univ. Kansas.
34. Archie GE (1942) The Electrical Resistivity Log as an Aid in Determining some Reservoir Characteristics. J Pet Technol 5: 54-62.
35. Doust H, Omatsola E (1989) Niger delta: AAPG Memoir 48: 201-238.